# Global characterization of optical power propagation in step-index plastic optical fibers

**Javier Mateo, M. Angeles Losada and Ignacio Garcés**

*GTF, Aragón Institute of Engineering Research (i3A), Department of Electronic Engineering, University of Zaragoza, María de Luna 1,50011Zaragoza, Spain*
*jmateo@unizar.es*

**Joseba Zubia**

*University of the Basque Country, Alda. Urquijo s/n, E-48013 Bilbao, Spain*

**Abstract:** We propose to characterize optical power transmission in step-index plastic optical fibers by estimating fiber diffusion and attenuation as functions of the propagation angle. We assume that power flow is described by Gloge´s differential equation and find a global solution that was fitted to experimental far field patterns registered using a CCD camera as a function of fiber length. The diffusion and attenuation functions obtained describe completely the fiber behavior and thus, along with the power flow equation, can be used to predict the optical power distribution for any condition.



**OCIS codes:** (060.0060) Fiber optics and optical communications; (060.2270) Fiber characterization; (060.2300) Fiber measurements; (060.2310) Fiber optics.

## References and links

1. G. Jiang, R. F. Shi, and A. F. Garito, "Mode coupling and equilibrium more distribution conditions in plastic optical fibers," IEEE Photon. Technol. Lett. **9,** 1128-1130 (1997).
2. W. A. Gambling, D. N. Payne, and H. Matsumura, "Mode conversion coefficients in Optical Fibers," Appl. Opt. **15**, 1538-1542 (1975).
3. J. Zubía, G. Durana, G. Aldabaldetreku, J. Arrúe, M. A. Losada, and M. López-Higuera, "New method to calculate mode conversion coefficients in SI multimode optical fibres," J. Lightwave Technol. **21**, 776-781 (2003).
4. M. A. Losada, I. Garcés, J. Mateo, I. Salinas, J. Lou and J. Zubía "Mode coupling contribution to radiation losses in curvatures for high and low numerical aperture plastic optical fibres," J. Lightwave Technol. **20**, 1160-1164 (2002).
5. R. Olshansky, and S. M. Oaks, "Differential mode attenuation measurements in graded-index fibers," Appl. Opt. **17**, 1830-1835 (1978).
6. T. Ishigure, M. Kano and Y. Koike, "Which is a more serious factor to the bandwidth of GI POF: differential mode attenuation or mode coupling?," J. Lightwave Technol. **18**, 959-965 (2000).
7. S. E. Golowich, W. White, W. A. Reed, and E. Knudsen, "Quantitative estimates of mode coupling and differential modal attenuation in perfluorinated graded-index plastic optical fiber," J. Lightwave Technol. **21**, 111–121 (2003).
8. D. Gloge, "Optical power flow in multimode fibers," Bell Syst. Tech. J. **51**, 1767-1783 (1972).
9. M. Rousseau, and L. Jeunhomme, "Numerical solution of the coupled-power equation in step-index optical fibers," IEEE Trans. Microwave Theory Technol. **25**, 577-585 (1977).
10. L. Jeunhomme, M. Fraise, and J. P. Pocholle, "Propagation model for long step-index optical fibers," Appl. Opt. **15**, 3040-3046 (1976).
11. A. Djordjevich, and S. Savovic, "Investigation of mode coupling in step index plastic optical fibers using the power flow Equation," IEEE Photon. Technol. Lett. **12**, 1489-1491 (2000).
12. A. Djordjevich, and S. Savovic, "Numerical solution of the power flow equation in step-index plastic optical fibers," J. Opt. Soc. Am. B **21**, 1437-1438 (2004).
13. S. Savovic, and A. Djordjevich, "Optical power flow in plastic-clad silica fibers," Appl. Opt. **41**, 7588-7591 (2002).

#71530 - $15.00 USD Received 31 May 2006; revised 6 September 2006; accepted 11 September 2006

14. N. Hashizume, E. Okugaki, S. Suyama, and M. Tatsutsuke, "Far field pattern measurement of POF in the presence of speckle noise," in *Proceedings of the International Conference on Plastic Optical Fibers and Application,* XII ed., Seattle, USA (2003).
15. M. A. Losada, J Mateo, D. Espinosa, I. Garcés and J. Zubia, "Characterisation of the far field pattern for plastic optical fibres," in *Procceedings of the International Conference on Plastic Optic Fibres and Application,* XIII ed., Nuremberg, Germany, (2004), pp. 458-465.
16. R. D. Skeel, and M. Berzins, "A Method for the Spatial Discretization of Parabolic Equations in One Space Variable," SIAM J. Sci. Stat. Comp. **11**, 1-32 (1990).
17. R. M. Lewis, and V. Torczon, "Pattern Search Algorithms for Bound Constrained Minimization," SIAM J. on Optimization **9**, 1082-1099 (1999).
18. M. A. Losada, J. Mateo, I. Garcés, J. Zubía, J. A. Casao, and P. Pérez-Vela, "Analysis of strained plastic optical fibres," IEEE Photon. Technol. Lett. **16**, 1513-1515 (2004).

## 1. Introduction

The shape of the far field pattern (FFP) of a plastic optical fiber (POF) is determined by the optical power distribution at the output of the fiber that depends on the initial distribution determined by launching conditions, on fiber properties, and naturally, on fiber length. Fiber properties involve power transfer among modes (modal coupling) and angular-dependent attenuation (differential attenuation), which are determined by the properties of the material, such as scattering and absorption, by the fiber intrinsic defects, and by external factors, like curvatures or the presence of a scrambler [1]. Power transfer between contiguous modes is generally quantified by the coupling strength, which depends on the coupling behavior of the fiber and has been estimated under several approximations [1-4]. Also, differential attenuation has been experimentally estimated for graded-index fibers in Refs. [5-7].

Gloge's power flow equation has been frequently used to describe the evolution of the modal power distribution as it is transmitted throughout a multimode fiber, where different modes are characterized by their propagation angle with respect to fiber axis [8]. The high number of modes transmitted inside a POF makes it possible to consider the propagation angle as a continuous variable ($\theta$). The diffusion equation can be solved analytically only in some particular cases [1, 3, 8], although a more general approach can be obtained using numerical methods [9-12]. In all these works, it is assumed that attenuation or diffusion or both have a constant value independent on the propagation angle. Here, we propose a more general model where both fiber diffusion and attenuation are described by angular functions: $D(\theta)$, and $\alpha(\theta)$, respectively, and for which a global solution is found.

With the aim to characterize optical power transmission in step-index plastic optical fibers (SI-POFs), we captured the FFP images for three SI-POFs of high numerical aperture (NA) as a function of fiber length. The longest measured length for each fiber was chosen to guarantee that the steady state power distribution (SSD) was reached. In our approach, a particular shape is proposed for the diffusion function, $D(\theta)$, with a few free parameters whose values are determined by minimizing the error between the model predictions and the experimental FFPs. Even more, we make no assumptions over the angular attenuation, $\alpha(\theta)$, which is calculated directly from the SSD and from the estimated diffusion function. We found that our estimated functions $D(\theta)$ and $\alpha(\theta)$ jointly with Gloge's power flow equation are able to reproduce the measured FFPs for the three fibers.

## 2. Theoretical modeling

The general diffusion equation that describes the optical power distribution, $P(\theta, z)$, in a multimode fiber as a function of fiber length ($z$) and of propagation inner angle with respect to fiber axis ($\theta$) is the following:

$$\frac{\partial P(\theta,z)}{\partial z} = -\alpha(\theta)P(\theta,z) + \frac{1}{\theta}\frac{\partial}{\partial\theta}\left(\theta D(\theta)\frac{\partial P(\theta,z)}{\partial\theta}\right). \quad (1)$$

#71530 - $15.00 USD Received 31 May 2006; revised 6 September 2006; accepted 11 September 2006

In Eq. (1), the power variation is accounted for by attenuation described by $\alpha(\theta)$ and by next-neighbor power diffusion described by $D(\theta)$. For large *z* values, when the angular power distribution has reached its SSD, the solution of the equation can be expressed as the product of two functions of independent variables:

$$P_{SSD} = Q(\theta)e^{-\gamma z}. \tag{2}$$

The function $Q(\theta)$ describes the shape of the SSD profile that depends only on the propagation angle, while the dependence on fiber length *z* is given by a decreasing exponential function which accounts for the power decrease due to the fiber attenuation $\gamma$. Introducing this solution into Eq. (1), an equation can be obtained relating: $\alpha(\theta)$, $Q(\theta)$ and $D(\theta)$. Thus, $\alpha(\theta)$ can be expressed in terms of the others as follows:

$$\alpha(\theta) = \gamma + \frac{1}{Q(\theta)\theta}\frac{\partial}{\partial\theta}\left(\theta D(\theta)\frac{\partial Q(\theta)}{\partial\theta}\right). \tag{3}$$

In this way, a shape for the attenuation function does not have to be assumed as it can be directly calculated provided $\gamma$, $Q(\theta)$ and $D(\theta)$ are known. On the other hand, although fiber diffusion has usually been modeled by a constant value in POFs [9-12], we use a more general function of the propagation angle as was done for plastic-clad silica fibers in [13].

We impose the more general boundary conditions for Eq. (1) which are the following:

$$\left.\frac{\partial P(\theta,z)}{\partial\theta}\right|_{\theta=0} = 0 \qquad P\left(\theta\to\frac{\pi}{2},z\right) = 0. \tag{4}$$

The first condition is necessary to prevent a singularity at $\theta = 0$ and its physical meaning is that there is no diffusion for the straight rays. The second condition indicates that there is no power propagating at high angles and, in most works, it was imposed for angles greater than the critical angle [11, 12]. However, we imposed it to the maximum measured angle based on our experimental evidence of tails in the FFPs indicating power propagation above the critical angle.

### 3. Experimental method to acquire FFP images and radial profiles

In this section we present the experimental set-up and methodology used to obtain the spatial distribution of the optical power as a function of the output propagation angle.

Three PMMA fibers of 1mm diameter from different manufacturers were tested: ESKA-PREMIER GH4001 (GH) from Mitsubishi, HFBR-RUS100 (HFB) from Agilent, and PGU-FB1000 (PGU) from Toray. The GH and PGU fibers have numerical aperture (NA) of 0.5 (corresponding to 19.5º inner critical angle) and 0.15dB/m of nominal attenuation. The HFB fiber has NA of 0.47 (18.5º inner critical angle) and 0.22dB/m of nominal attenuation.

The procedure used to characterize the fibers was the following: We started with the whole length of the fiber to test rolled onto an 18cm diameter reel. The input end of the fiber was connected to a transmitter based on an AlGaInP laser diode (LD SANYO DL-3147-021) emitting 5mW at 645nm and with a typical divergence of 30º in the perpendicular plane, and of 7.5º in the parallel plane. The FFP image reflected on a white screen placed opposite the fiber output end was taken using a 12 bit monochrome cooled camera QICAM FAST 1394. Then, a segment of 10m/5m/2.5m was cut from the input end of the fiber and the whole procedure started again, up to 10m. The longest measured length for each fiber was chosen to guarantee that the SSD had been reached. It was 175m for the GH fiber, 100m for the HFB and 150m for the PGU. The speckle noise was minimized with a mechanical vibration generated by an external motor and applied to the fiber near the input end [14]. Further details of the method to obtain the FFPs were explained elsewhere [15]. Figure 1 shows a scheme of the set up, the screen of the custom program to acquire the FFP and the radial profiles and a picture of the FFP projected over the screen.

#71530 - $15.00 USD Received 31 May 2006; revised 6 September 2006; accepted 11 September 2006

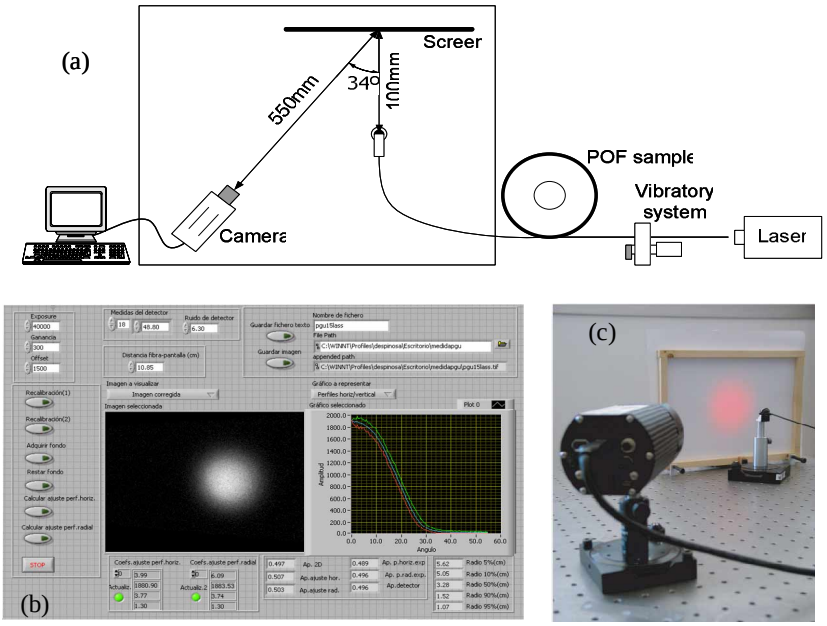


Fig. 1. (a). Scheme of the set up. (b) Screen of the custom program to acquire the FFP and radial profiles. (c) Picture of the set up showing the FFP over the screen.

Figure 2 shows as an example the images registered at the output of 10m, 50m and 150m of the GH fiber. The relationship between the image scale in pixels and the internal angle is given by simple geometry and Snell Laws. Thus, the maximum measured internal angle was 33.6º, corresponding to an external angle of 55.6º, well above the theoretical external critical angle for these fibers which is 30º. From the raw images the centroid was obtained and the radial profile, shown below in Fig. 2, was calculated by averaging the values of all the pixels at a given distance from it. The differences in the FFPs at different fiber lengths can be better appreciated by comparing these profiles. As we have under-filled launching, the profile at 10m is the narrowest. At 50m, the power has spread to higher angles and the pattern is wider. Finally, at 150m the pattern is practically the SSD. From it, a NA close to the manufacturer value of 0.5 can be obtained.

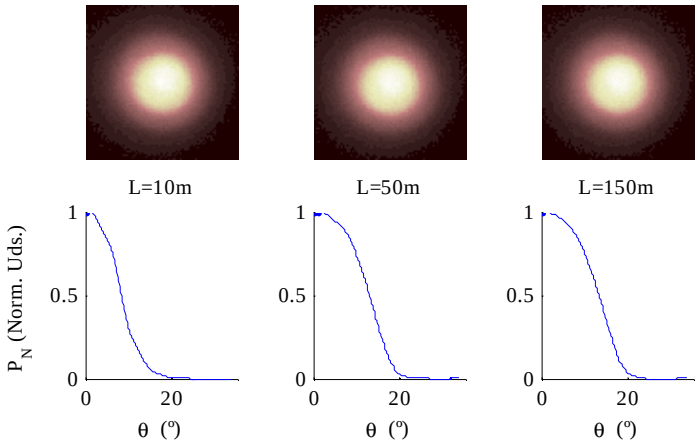


Fig. 2. Images of the far field pattern for the GH fiber at 10m, 50m and 150m acquired with the CCD and their corresponding calculated radial profiles.

#71530 - $15.00 USD Received 31 May 2006; revised 6 September 2006; accepted 11 September 2006

## 4. Fiber characterization method and results

In this section, we describe our procedure to characterize power propagation in POFs by obtaining the diffusion and attenuation functions. Equation (3) allows to calculate attenuation provided $\gamma$, $Q(\theta)$ and $D(\theta)$ are known. Thus, in the first subsection we describe how we estimate $\gamma$ directly from our experimental data. In the second subsection, the experimental SSDs are fitted by a sigmoid-like function of the squared propagation angle to obtain an analytical form of $Q(\theta)$ and its derivatives. In the last subsection, we estimate fiber diffusion by modeling $D(\theta)$ both by a constant and a sigmoid function.

### *4.1 Estimation of attenuation $\gamma$*

The fiber attenuation was calculated from the total power obtained from the profiles of the measured FFP images as the integral over the full solid angle following the next expression:

$$P_T(z) = \int_{\Omega f} P(\theta, z) d\Omega = \int_0^{2\pi} d\varphi \int_0^{\frac{\pi}{2}} \sin(\theta) P(\theta, z) d\theta = 2\pi \int_0^{\frac{\pi}{2}} \sin(\theta) P(\theta, z) d\theta . \qquad (5)$$

In Fig. 3(a) $\ln(P_T(z))$ is represented as a function of fiber length for the three fibers. The values of the attenuation $\gamma$ for each fiber are obtained from the slopes and they are given in Table 1.

### *4.2 Bi-sigmoid fits to the steady state profiles*

In order to obtain the angular attenuation using Eq. (3), we have to provide an analytical expression for $Q(\theta)$ and for its derivatives. Thus, the normalized SSDs for the three fibers were fitted by a product of two sigmoid functions of the squared inner angle, given by:

$$Q_N(\theta) = \frac{\left(1+e^{-\sigma_1^2\theta_1^2}\right)\left(1+e^{-\sigma_2^2\theta_2^2}\right)}{\left(1+e^{-\sigma_1^2\left(\theta_1^2-\theta^2\right)}\right)\left(1+e^{-\sigma_2^2\left(\theta_2^2-\theta^2\right)}\right)} . \qquad (6)$$

This function has several characteristics that make it very suitable for our purposes: It has a flat asymptotic behavior at the origin and at infinity, it decreases monotonically and it is even and continuously derivable. In addition, the four free parameters that characterize these functions give sufficient flexibility to model the different slopes of the head and the tails of the FFPs. Indeed, these functions can be used to fit the FFPs at all lengths with smaller error than by using super Gaussian functions as was done in a previous work [15]. The values of the parameters that best fit the SSDs are given in Table 1, as well as the root mean square error (RMSE) for the three fibers. The goodness of the fits can be observed in Fig. 3(b) where they are displayed as lines along with the original data as symbols for the three fibers tested. Notice the presence of power beyond the inner critical angle (19º) for all fibers whose SSDs are very similar which is not surprising as they have similar optical configuration.

Table 1. Attenuation $\gamma$ and $Q_N(\theta)$ parameters for the best fits to the SSD of the three fibers

| | $\gamma$ | | $Q_N(\theta)$ [a] | | | | |
|---|---|---|---|---|---|---|---|
| Fiber | *np/m* | *dB/m* | $\sigma_1$ | $\theta_1$ | $\sigma_2$ | $\theta_2$ | *RMSE* |
| GH | 0.0331 | 0.1438 | 6.5327 | 0.2689 | 4.0744 | 0.2689 | $2.479\times10^{-3}$ |
| HFB | 0.0344 | 0.1496 | 6.1991 | 0.2651 | 3.9867 | 0.2651 | $5.517\times10^{-3}$ |
| PGU | 0.0404 | 0.1754 | 6.4475 | 0.3275 | 5.1740 | 0.1920 | $2.578\times10^{-3}$ |

[a] Defined in Eq. (6).

#71530 - $15.00 USD Received 31 May 2006; revised 6 September 2006; accepted 11 September 2006

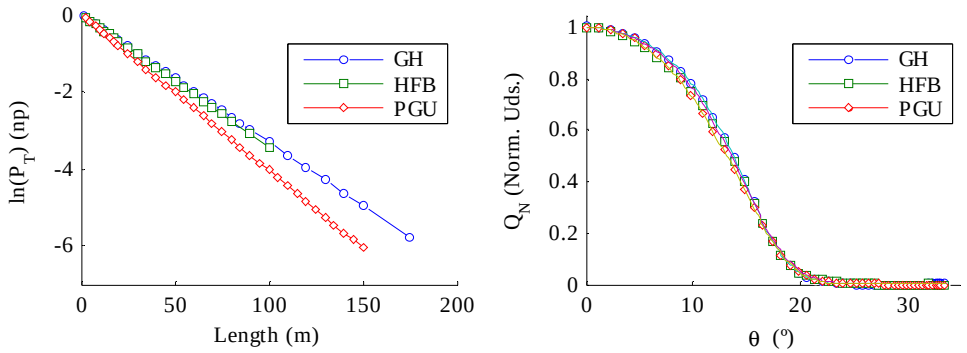


(a) Total power versus fiber length

(b) Radial profile of the SSD

Fig. 3. Total power versus length and SSD radial profiles for the three tested fibers: GH data is shown as circles and (blue) lines; HFB as squares and (green) lines, and PGU as diamonds and (red) lines. In Fig. 3(b) data symbols represent the raw data from the radial profiles and the lines give the best-fit to Eq. (6).

*4.3 Determination of the diffusion function*

To estimate $D(\theta)$, we solve numerically Eq. (1) [16] to obtain the model predictions for the FFP profiles starting with a guess for $D(\theta)$. The final estimate of $D(\theta)$ is the one that minimize the RMSE between the measured FFPs and the model predictions. We use a direct search pattern method [17] to find a global minimum in the objective RMSE function. In each iteration, the latest estimate of $D(\theta)$ is introduced in Eq. (3) to calculate the corresponding attenuation function $\alpha(\theta)$.

In the first approach, the diffusion function is modeled by a constant $D_c$ as it is usually assumed [9-12]. Table 2 shows the values of $D_c$ and the RMSE for the best fit for the three fibers. Fig. 4(a) shows the radial profiles for the GH fiber at several lengths. The comparison between the measured and the predicted profiles shows how, in the intermediate lengths, the power at small angles is underestimated, while at larger angles power it is overestimated suggesting that diffusion should be higher at small angles than at larger ones. This fact justifies our proposal to model fiber diffusion by a function of propagation angle. We chose a sigmoid function of the squared inner angle because of its mathematical properties, although other similar function could be used. This function is given by the following expression:

$$D(\theta) = D_0 + \frac{D_1}{1 + D_2 e^{\sigma_d^2 \theta^2}}, \tag{7}$$

where $D_0$, $D_1$, $D_2$, and $\sigma_d$ are free parameters of our model. The value of this function at small angles tends to $D_0 + D_1/(1+D_2)$ while for larger angles tends to $D_0$. The position and magnitude of the slope are governed jointly by $D_2$ and $\sigma_d$. The model predictions for the GH fiber are shown in Fig. 4(b) displaying a considerably better agreement than was found previously for a constant diffusion model.

The values of the parameters that characterize the diffusion function for the two different approaches and their corresponding errors in predicting the FFPs are shown in Table 2. The sigmoid diffusion functions calculated introducing these parameters into Eq. (7) and the attenuation functions derived from Eq. (3) are represented in Fig. 5(a) and Fig. 5(b) respectively for the three fibers.

#71530 - $15.00 USD Received 31 May 2006; revised 6 September 2006; accepted 11 September 2006

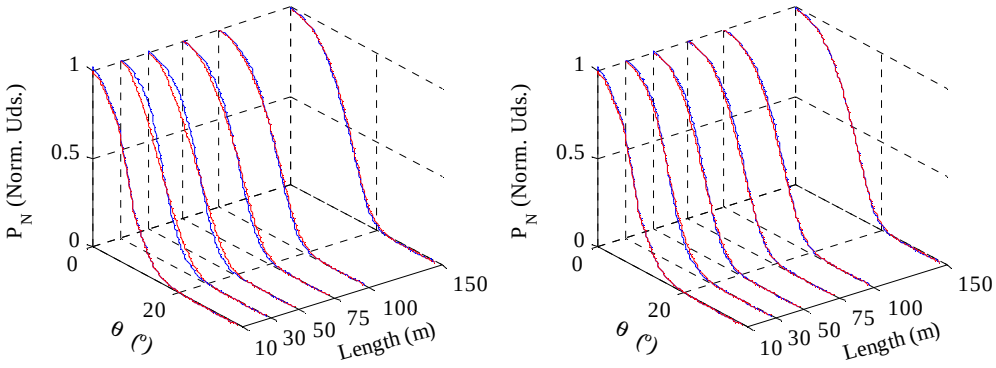


(a) Constant diffusion model (b) Sigmoid diffusion model

Fig. 4. Experimental radial profiles (blue lines) for the GH fiber at 10, 30, 50, 75, 100 and 150m are shown in both graphs along with those predicted by both models (red lines).

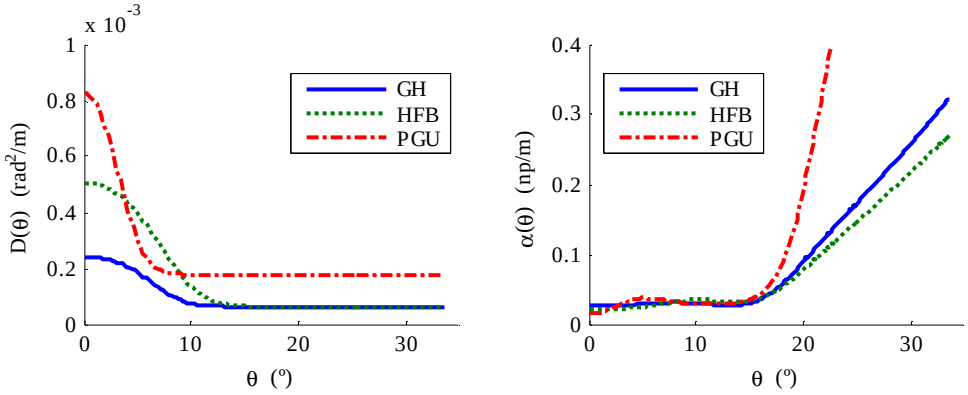


(a) Diffusion functions (b) Attenuation functions

Fig. 5. Diffusion and attenuation functions for the three fibers obtained by modeling diffusion with the sigmoid function given by Eq. (9). GH fiber results are shown as blue solid lines, HFB fiber results as green dashed lines and PGU fiber results as red dash-dotted lines.

Table 2. Parameters for the constant diffusion and sigmoid diffusion functions that minimizes the error between experimental and model-predicted far field profiles.

| | $D_c$ | | $D(\theta)$ [a] | | | | |
|---|---|---|---|---|---|---|---|
| Fiber | $rad^2/m$ | *RMSE* | $D_0$ | $D_1$ | $D_2$ | $\sigma_d$ | *RMSE* |
| GH | $1.171\times10^{-4}$ | $22.7\times10^{-3}$ | $6.356\times10^{-5}$ | $2.338\times10^{-4}$ | 0.321 | 11.66 | $16.4\times10^{-3}$ |
| HFB | $1.649\times10^{-4}$ | $17.1\times10^{-3}$ | $6.196\times10^{-5}$ | $6.513\times10^{-4}$ | 0.466 | 9.626 | $8.45\times10^{-3}$ |
| PGU | $2.271\times10^{-4}$ | $12.9\times10^{-3}$ | $1.775\times10^{-4}$ | $1.561\times10^{-3}$ | 1.403 | 16.54 | $8.92\times10^{-3}$ |

[a] Defined in Eq. (7).

#71530 - $15.00 USD Received 31 May 2006; revised 6 September 2006; accepted 11 September 2006

## 5. Discussion

The experimentally observed behavior of power propagation throughout SI-POFs is better described by modeling diffusion with sigmoid functions, since power spread towards higher angles is stronger for lower than for higher angles as Fig. 4 shows. Our condition of under-filled launching has been chosen because it is customary in actual systems, particularly, when bandwidth is a requirement. Also, this condition is suitable for our method to characterize the fibers using FFPs measurements as it allows diffusion to act spreading optical power, particularly at short fiber lengths, and thus, provides information about the diffusion function that we want to obtain. The attenuation and diffusion functions estimated for our particular experimental conditions describe fiber intrinsic properties that should be applicable to other launching conditions. We found that power diffusion is the most important factor at short fiber lengths. At longer fiber lengths, the combination of diffusion and attenuation smoothes the tails producing a stable shape as the SSD is being reached. Angular attenuation is the most influent factor at the longest lengths, determining the shape of the SSD.

Our results in Fig. 5 show significant differences in both the diffusion and attenuation functions for the three different fibers. The diffusion functions show a decrease for angles well below the critical angle, tending to an asymptotic value which is inherent to the sigmoid function used to model diffusion in our proposal. In any case, the value of the diffusion function near the critical angle is not significant because attenuation is dominant for these angles. According to our results, the GH fiber has the least and the flattest diffusion. On the other hand, for the PGU the diffusion is the highest and the steepest one.

The attenuation functions are relatively flat for the lower angles and rise steeply near the critical angle. There is not, however, such an abrupt increase at exactly the critical angle as postulated in other works [2, 9, 11]. Differences among fibers in the flat region of the attenuation function are mainly due to the different values of $\gamma$, although there are also some ripples that could be explained by the different behavior of the fibers under the curvatures of the reel [4]. For the PGU fiber, the obtained attenuation $\gamma$ is quite higher than its nominal attenuation and also this fiber exhibits the highest diffusion. This behavior suggests that the tested PGU sample was probably strained. In fact, it was shown [18] that the effect of strain is to increase fiber attenuation and power diffusion.

The presence of power above the critical angle in the experimental patterns indicates that light paths exist beyond the critical angle, which cannot be reproduced if the attenuation is described by a function whose value is infinity just above the critical angle. In fact, our estimated attenuation does not rise abruptly at the critical angle but increases smoothly in its neighborhood. This behavior could be explained by understanding the critical angle as a randomly distributed variable along the fiber rather than a single deterministic value physically originated by fiber distributed in-homogeneities, curvatures and leaky ray paths. The slope rising above the critical angle is different for the three fibers since it is determined by the asymptotic value of the diffusion function. However, its value hardly affects the model predictions as in this region there is very low optical power.

## 5. Conclusion

We have presented a model for power transmission in step-index plastic optical fibers that permits to describe fiber diffusion and attenuation by means of more generalized functions of the propagation angle. These two functions along with the diffusion differential equation provide a complete description of the process of power propagation throughout the fiber, and can be used to predict the FFP under different launching conditions and to estimate other parameters of interest such as steady state length, attenuation, bandwidth, etc.

## Acknowledgments

This work was supported by the University of the Basque Country and the Basque Government under projects GIU05/03, UE05/A25, HEGATEK-05, SENSOFIB/SAIOTEK and by the Spanish Ministry for Science and Technology under grant TIC2003-08361.

#71530 - $15.00 USD Received 31 May 2006; revised 6 September 2006; accepted 11 September 2006